Heuristically optimal path scanning for high-speed multiphoton circuit imaging

Alexander J. Sadovsky, Peter B. Kruskal, Joseph M. Kimmel, Jared Ostmeyer, Florian B. Neubauer and Jason N. MacLean

J Neurophysiol 106:1591-1598, 2011. First published 29 June 2011; doi:10.1152/jn.00334.2011

Journal of Neurophysiology publishes original articles on the function of the nervous system. It is published 12 times a year (monthly) by the American Physiological Society, 9650 Rockville Pike, Bethesda MD 20814-3991. ISSN: 0022-3077, ESSN: 1522-1598. Visit our website at http://www.the-aps.org/.

J Neurophysiol 106: 1591–1598, 2011.
First published June 29, 2011; doi:10.1152/jn.00334.2011.

Heuristically optimal path scanning for high-speed multiphoton circuit imaging

Alexander J. Sadovsky,* Peter B. Kruskal,* Joseph M. Kimmel,* Jared Ostmeyer, Florian B. Neubauer, and Jason N. MacLean
Department of Neurobiology, University of Chicago, Chicago, Illinois

Submitted 14 April 2011; accepted in final form 22 June 2011

Sadovsky AJ, Kruskal PB, Kimmel JM, Ostmeyer J, Neubauer FB, MacLean JN. Heuristically optimal path scanning for high-speed multiphoton circuit imaging. *J Neurophysiol* 106: 1591–1598, 2011. First published June 29, 2011; doi:10.1152/jn.00334.2011.—Population dynamics of patterned neuronal firing are fundamental to information processing in the brain. Multiphoton microscopy in combination with calcium indicator dyes allows circuit dynamics to be imaged with single-neuron resolution. However, the temporal resolution of fluorescent measures is constrained by the imaging frequency imposed by standard raster scanning techniques. As a result, traditional raster scans limit the ability to detect the relative timing of action potentials in the imaged neuronal population. To maximize the speed of fluorescence measures from large populations of neurons using a standard multiphoton laser scanning microscope (MPLSM) setup, we have developed heuristically optimal path scanning (HOPS). HOPS optimizes the laser travel path length, and thus the temporal resolution of neuronal fluorescent measures, using standard galvanometer scan mirrors. Minimizing the scan path alone is insufficient for prolonged high-speed imaging of neuronal populations. Path stability and the signal-to-noise ratio become increasingly important factors as scan rates increase. HOPS addresses this by characterizing the scan mirror galvanometers to achieve prolonged path stability. In addition, the neuronal dwell time is optimized to sharpen the detection of action potentials while maximizing scan rate. The combination of shortest path calculation and minimization of mirror positioning time allows us to optically monitor a population of neurons in a field of view at high rates with single-spike resolution, ~125 Hz for 50 neurons and ~8.5 Hz for 1,000 neurons. Our approach introduces an accessible method for rapid imaging of large neuronal populations using traditional MPLSMs, facilitating new insights into neuronal circuit dynamics.

calcium imaging; multiphoton microscopy; neuronal dynamics; software

LOCAL POPULATIONS OF NEURONS code and store information through patterned neuronal activations (Harris 2005; Hebb 1949; Kudrimoti et al. 1999). Spatiotemporal patterns of neuronal activation are readily observed using calcium indicator dyes (MacLean et al. 2005; Ohki et al. 2006; Watson et al. 2008). The high spatial resolution of multiphoton laser scanning microscopy (MPLSM) allows for the recording of fluorescence from potentially thousands of neurons with single-cell resolution. However, the sequential pixel by pixel sampling of a field of view imposes a severe limit on the temporal resolution of a full scan or frame and thus lessens the ability to accurately detect the temporal sequences of action potential generation in a population of neurons.

Recognizing this limitation, researchers have improved the hardware associated with MPLSM. These recent innovations increase the rate of MPLSM fluorescence measures using specialized beam-steering hardware for faster laser scanning, including acousto-optical devices (AODs) (Duemani Reddy et al. 2008; Göbel et al. 2007; Otsu et al. 2008) and resonant galvanometer mirrors (Cheng et al. 2011; Fan et al. 1999). Other hardware-based techniques increase multiphoton temporal resolution by breaking the incident beam into multiple scan beams through diffractive optical elements (Watson et al. 2009) and spatial light modulators (SLM) (Nikolenko et al. 2008). Although both of these families of approaches are able to significantly increase scan speed, they require the user to purchase equipment not found on a standard multiphoton microscope. In addition, AOD and SLM technologies restrict the number of neurons that can be monitored due to either small limited scan angles or upper bounds on the total number of beamlets, respectively.

Improvements have also been made in the software used to optimize scanning. One approach is to increase mirror travel speed by maximizing velocity while moving over a user-generated path (Lillis et al. 2008). This approach allows an experimenter to select which areas to scan and then optimizes the physical mirror constraints to reach these regions. A different method, the vector mode approach (Nikolenko et al. 2007), automates both cell detection and scan path creation. This approach is ideal for circuit mapping using caged compounds. Another recent method has combined automated cell detection and an ant colony optimization path-finding algorithm for imaging populations of 50 neurons (Valmianski et al. 2010). To date, no MPLSM path construction algorithm has addressed the necessity for scalability to large numbers of targets, the ability to create optimal paths in a matter of seconds, and the need to optimize the physical movement of the scan mirror galvanometers for path stability within a single software suite.

To maximize the speed of fluorescence measurement from large populations of neurons using a standard MPLSM setup, we have developed heuristically optimal path scanning (HOPS), which provides user parameter-controlled and computationally optimized scans of many targets. Each part of HOPS can be independently accessed by the user, allowing for easy integration into current experimental designs. HOPS algorithmically minimizes the laser scan path using high-speed open-source TSP software that currently holds the record for computing paths with unknown optima. In addition, HOPS

* A. J. Sadovsky, P. B. Kruskal, and J. M. Kimmel contributed equally to this work.

Address for reprint requests and other correspondence: J. N. MacLean, Dept. of Neurobiology, Univ. of Chicago, Chicago, IL 60637 (e-mail: jmaclean@uchicago.edu).

includes characterization of the scan mirror galvanometers to achieve prolonged path stability. To sharpen the detection of action potentials, HOPS also optimizes the laser dwell time on individual neurons. Finally, HOPS rapidly automates each step of its process from the initial scan to the output of a neuronal fluorescence time series.

METHODS

Preparation of Acute Slices

C57BL/6 mice of postnatal *days 14–21* were used to generate thalamocortical slices with a vibratome (VT1000S). Mice were anesthetized by intraperitoneal injection of ketamine-xylazine. All procedures were approved by the Institutional Animal Care and Use Committee at the University of Chicago.

Electrophysiology

Whole cell current-clamp recordings and current pulse injections were made using Multiclamp 700B amplifiers (Axon Instruments).

MPLSM

Images of fura-2 AM bulk-loaded neurons were acquired with a custom-built multiphoton microscope using a femtosecond-pulsed Chameleon Ultra II Ti:sapphire laser (Coherent; $\lambda = 790$ nm). The objective ($\times$20, 0.95 NA) and BX50WI microscope body was obtained from Olympus. Scan mirrors (model 6210H) were obtained from Cambridge Technologies, and the photomultiplier tube (PMT) was acquired from Hamamatsu. Galvomotors were given voltage commands at 312.5 kHz via a DAQ board (model 6733; National Instruments) and custom software.

HOPS Software

HOPS is licensed under a Creative Commons noncommercial ShareAlike license; source code can be downloaded at http://macleanlab.uchicago.edu/software/. Raster images were collected via custom-written software and saved as 16-bit TIFF files (LabView). These images were processed by a custom software suite (Python), which performed automatic, user-editable detection of neural somata. The centroids of these somata were then output by the Python software in the text file format required by the TSP-solver, Lin-Kernighan heuristic (LKH; http://www.akira.ruc.dk/~keld/research/LKH/). LKH then found either the true optimal or a nearly optimal order in which to visit the cell centroids. This information was read back in by the Python suite and converted to a series of voltage commands using a pregenerated mirror lookup table (see RESULTS). Path information was read in by custom-written C# code linked against the National Instruments DAQmx data acquisition library. We used DAQmx to construct a three-channel task. One channel outputs an analog square pulse "TTL" (transistor-transistor logic) at the head of each laser tour for synchronization with electrophysiological data. The other two channels are the mirror voltage commands that define the laser's tour. This output task is then spooled continuously with no lag until a user-set timer is triggered and data acquisition stops. After data acquisition, the C# software parses the collected data into a plain text file with the average fluorescence observed in each cell from each iteration of the laser's tour. Each step in the software is completely modular and independent. Image acquisition, cell detection, TSP generation, scan path generation, and scan implementation are linked together via flat text file input/output, and as a result any module can be replaced by commercial or user-generated software. In addition, any part can be accessed independently of the rest of HOPS by creating data in this format. More details can be found in the readme.txt file included in the software package.

Path Optimality

The optimal, shortest path length was found using the Concorde travelling salesman problem solver (http://www.tsp.gatech.edu/concorde.html).

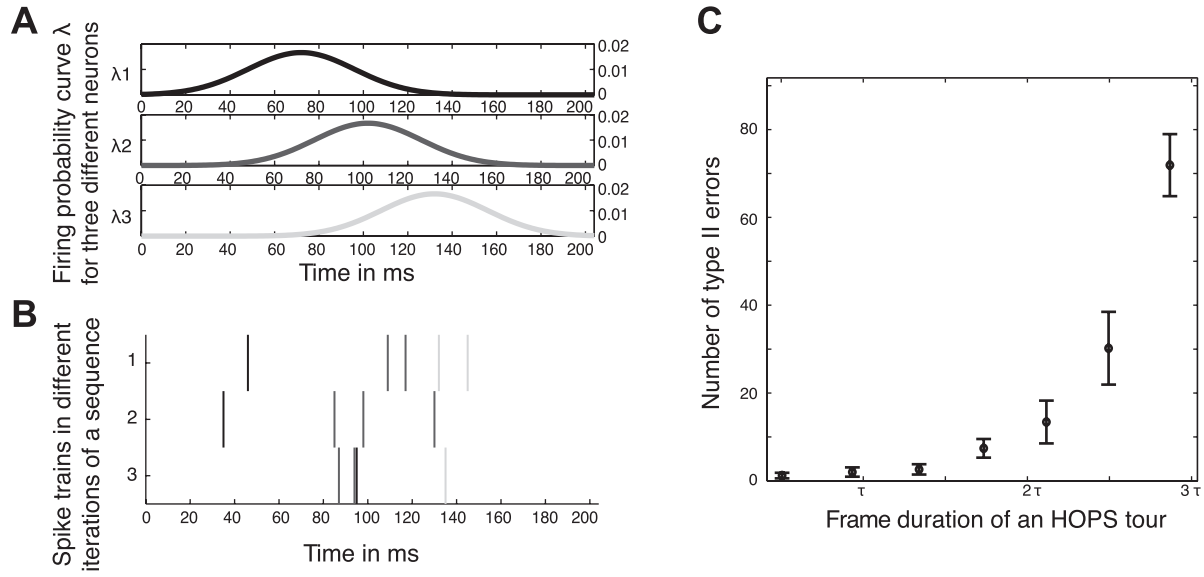

Fig. 1. Model for the generation of artificial spike trains that quantifies the improvement of single-action potential recovery from large-scale calcium imaging data as provided by heuristically optimal path scanning (HOPS). *A*: probability of a spiking event, $\lambda(t)$, follows a Gaussian curve with a peak at some increment of a temporal resolution $\tau = 30 \pm 24$ ms. Separate neurons overlap in their probabilities of firing at different times (denoted as 3 differently shaded lines). *B*: an example of 3 spike train sequences of 3 neurons generated from the model. Every millisecond, a spike is assigned with probability $\lambda(t)$, shown in *A*. *C*: the duration of a scan affects our ability to distinguish the temporal structure of a neuronal sequence in which the maximal correlation between neuronal firing occurs at some lag in increments of τ. Distinguishing temporal order among 1,000 artificial neurons following a sequence with temporal resolution τ, we find that the number of type II errors increases with the scan time. Values are means; error bars represent $\pm$SD.

Analysis of Scan Rate and Type II Errors

To test the effect of the duration of a HOPS tour on the detection of temporal sequences from Ca^{2+} data, we generated artificial spike train data with a fixed temporal structure. Sparse spike trains (1,000) were generated from an inhomogeneous Bernoulli process by which every millisecond, a spike could be generated with probability λ, where λ varied across time. $\lambda(t)$ followed a Gaussian curve with a standard deviation of 0.8τ so that, on average, every neuron fired one spike. Temporal structure was established by shifting the center times of these Gaussians by increments of some temporal resolution τ that defines a sequence for the network (Fig. 1*A*). From this, we obtained a set of spike trains S with a fixed temporal structure based on τ. We then generated several sets ($n = 30$) of these spike trains following the same neuronal sequence (Fig. 1*B*). We evaluated our ability to detect temporal structure by approximating the actual spike trains, S, with our estimate, $\hat{S}$, where $\hat{S}$ is a discretized spike train with bin widths equal to the time of a given HOPS tour. This lets $\hat{S}$ be analogous to the type of data collected in a Ca^{2+} imaging experiment. We then performed a *t*-test between the spike timing between every pair of neurons using the simulated spike times. If timing differences between a neuron pair were significant ($P < 0.05$ with $n = 30$ sequences), we assigned them the appropriate order in a sequence. If a pair was not significant, we assigned them to the same temporal position in the sequence. We then compared the estimate of the sequence order with the actual sequence order known from the probability functions $\lambda(t)$. Specifically, we counted the number of type II errors in looking for temporal structure as a function of scan rate (Fig. 1*C*, $\tau = 30$ ms). Without loss of generality, we considered scan rate as a function of τ and evaluated the level of temporal discriminability given this rate. Since HOPS allows us to modify the scan rate on the fly by dropping targets, we can adjust our path to always maintain a given level of temporal resolution. All statistics are means ± SD and were performed in MATLAB or Python.

RESULTS

Our goal with HOPS was to image as large a population of neurons as quickly as possible. We set out to create a MPLSM

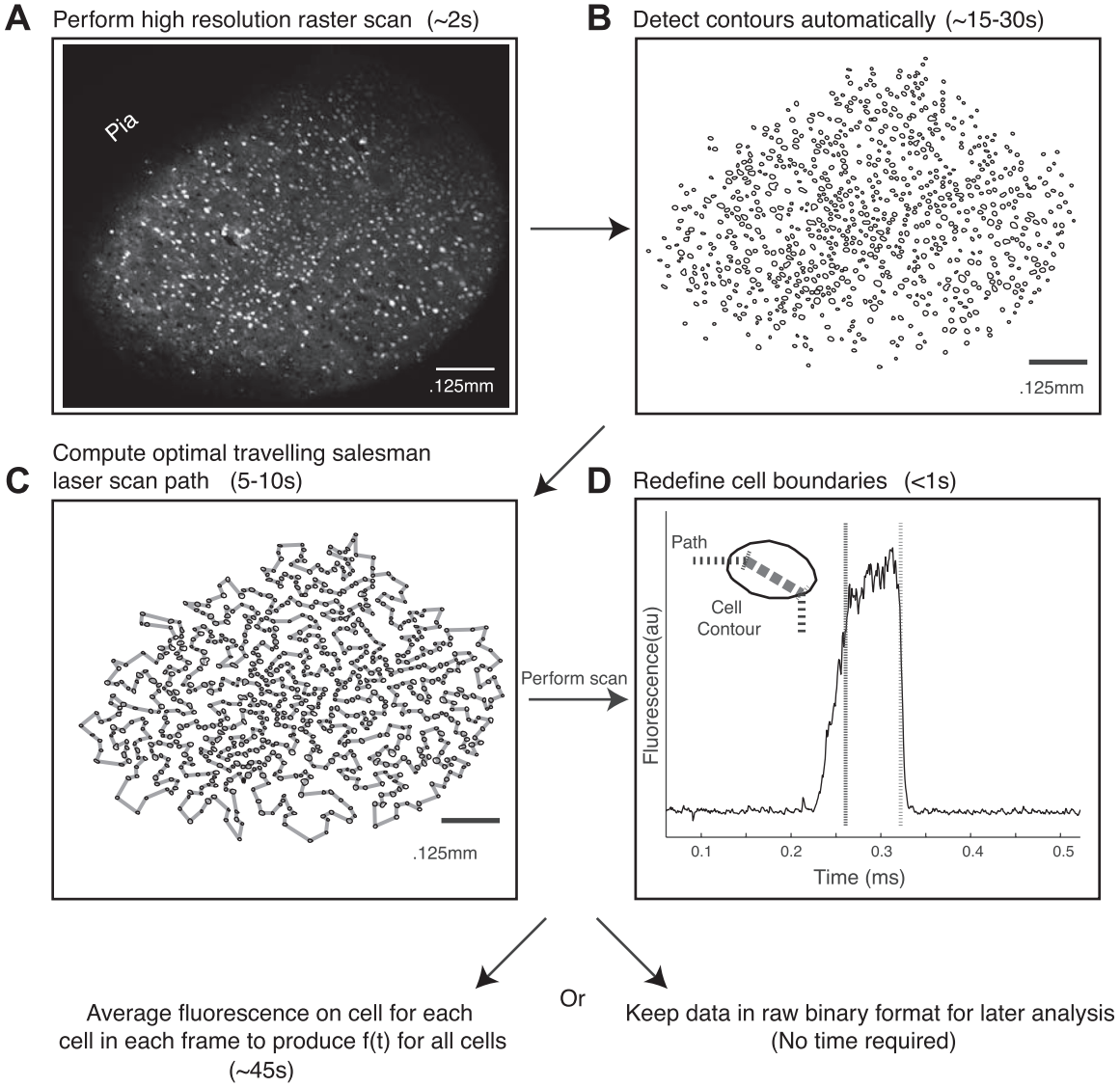

Fig. 2. Experimental flow from the initial raster scan to high-speed imaging including expectations for the computation time of each step. *A*: high-resolution multiphoton laser scanning microscopy (MPLSM) of fura-2 AM-loaded neurons in a slice of mouse somatosensory cortex. Bright punctuate areas are cell somata (1,365 detected). *B*: neurons are automatically detected using a set of filters, and a contour for each neuron is computed. *C*: a near-optimal path is generated using Helsgaun's open-source implementation of the Lin-Kernighan heuristic algorithm. Frame duration, 110.8192 ms/frame. *D*: cell boundaries are redefined from the raw fluorescence trace acquired during HOPS to make optimal use of all fluorescence samples collected on cell.

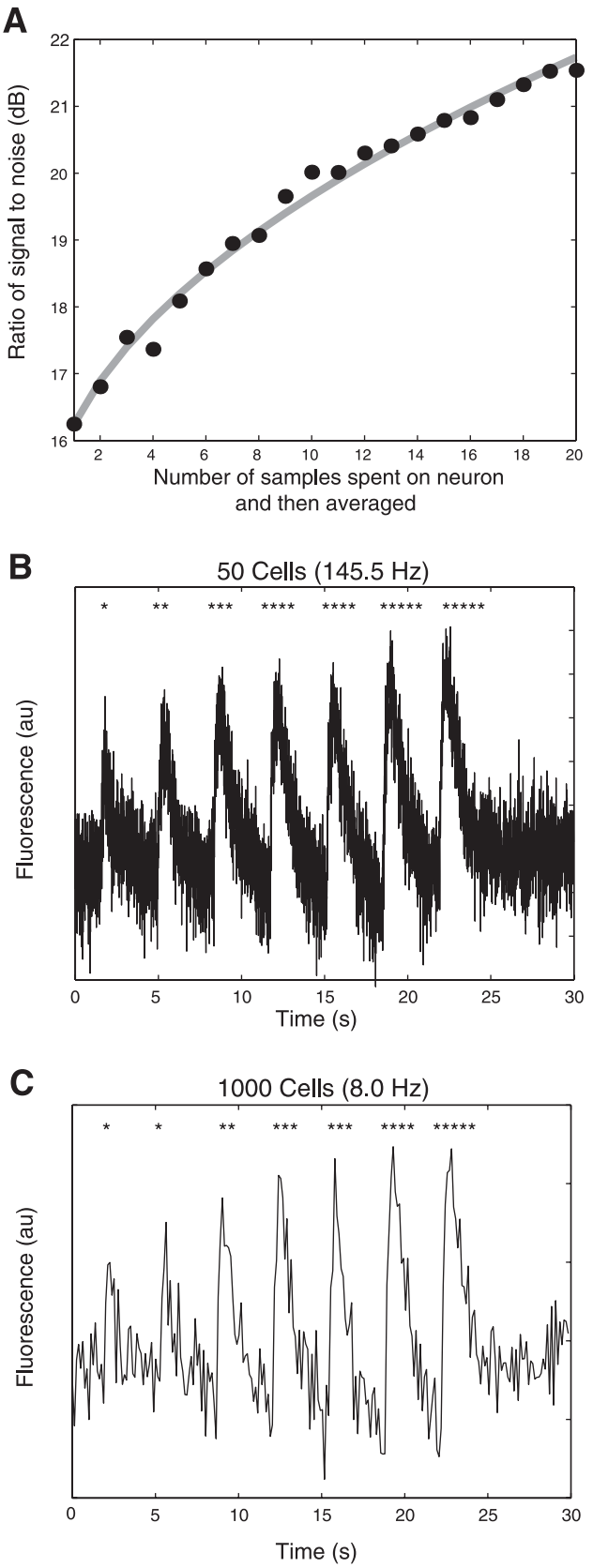

path optimization software package that requires minimal user intervention; runs online and thus quickly generates the optimal scan path; balances scan speed, scan stability, and signal quality; does not require additional specialized hardware; and is compatible with custom software packages used in most neuroscience laboratories.

Functional Importance

During MPLSM the ability to resolve the timing difference of action potential generation between two cells is a direct consequence of the frame rate of the scan. This is important for determining temporal sequence structure in neuronal data, a common question in many experiments. To evaluate the tradeoff between scan speed and sequence detection, we first generated 1,000 sparse spike trains from inhomogeneous Bernoulli processes with a specified temporal structure defined by τ (see METHODS, Fig. 1*A*). We generated several sets ($n = 30$) of these spike trains following the same neuronal sequence so that we could evaluate our ability to detect temporal structure (Fig. 1*B*). Specifically, we counted the number of type II errors when looking for temporal structure as a function of scan rate. We found that the number of type II errors in the detection of circuit sequences increases as frame duration increases (Fig. 1*C*, $\tau = 30$ ms). With scan rates faster than τ, the number of type II errors is negligible; however, there is a substantial increase with multiples greater than 2τ. As scan rates slow beyond 2τ, it becomes increasingly likely that sequences present are not detected. However, the model also indicates that even small increases in scan speed can lead to a significant improvement in the ability of a researcher to resolve the timing difference in action potential generation. Using HOPS to increase frame rate enables greater detection of neuronal firing sequences, especially in large populations of neurons.

Experimental Flow

Cell detection. The initial step of HOPS is the generation of a high-resolution (800 × 800 pixel) raster image of the calcium indicator-loaded tissue (Fig. 2*A*). We then automatically detect neurons from the initial scan: The raster is smoothed using a Gaussian filter, and cell contours are detected using a donut-shaped two-dimensional filter with widths matching an average cell diameter for a specific objective (Fig. 2*B*), similar to a previous report (Nikolenko et al. 2007). The image is then resmoothed and thresholded based on fluorescence values to detect individual cells. Contours are then checked for circularity by testing how well they approximate π. If a contour is not circular, it is assumed to be multiple cells and is recursively

Fig. 3. Optimizing signal-to-noise ratio permits single-action potential generation. *A*: illustrative example of single event noise at different numbers of samples collected and then averaged from each cell. The final fluorescence intensity measure for each neuron for each frame is plotted according to samples on cell. Shaded line is a theoretical fit to the model $Y = A \cdot (1/\sqrt{X}) + C$, where $A = 1.584$ and $C = 14.65$. R^2 of the fit with the data is 0.9888. *B*: changes in fluorescence indicate action potential generation. A neuron was patched and 1–5 action potentials (number indicated by asterisks) were evoked via brief injections of current during HOPS acquisition of 50 cells at 145.5 Hz. The trace was filtered with a high-pass Butterworth filter to remove trending. *C*: action potential detection via fluorescence from a large-population HOPS scan. As in *B*, a neuron was patched and action potentials were evoked via brief injections of current during HOPS acquisition of 1,000 cells at 8.0 Hz. The trace was filtered in the same manner as in *B*.

split, and each resulting contour is again checked for circularity. The user then has the ability to add or delete erroneous contours; however, the necessary amount of modification is minimal, usually resulting in at most 1–2% of the population having type I and II errors in detection. After cell identification, a list of the centroids of each contour is compiled to be fed into the path determination algorithm. For an alternative approach for cell detection using supervised learning algorithms, which can also be utilized in combination with HOPS, see Valmianski et al. 2010.

Optimal TSP implementation. For path construction, HOPS utilizes K. Helsgaun's implementation of the LKH (Helsgaun 2000) approach to the travelling salesman problem. An optimal or near-optimal path is constructed so that HOPS can visit each neuron once per tour while minimizing interneuron travel time (Fig. 2*C*). This low-level ANSI C software has been widely used, for instance, in radiation hybrid genomic mapping (Amaral et al. 2008) and wireless sensor network energy-saving approaches (Apiletti et al. 2010) and has proved itself effective in TSP contests. LKH is an ideal software solution for our path creation purposes because it rapidly calculates paths (in under 10 s) and is highly scalable (1,000+ neurons). In our setup, using 846 neurons as a benchmark, the optimal path was found on average in 3.1 s in 962 of 1,000 runs. The 38 nonoptimal path calculations were only 1 path unit suboptimal, which, given the average path length, corresponds to a negligible increase of a few microseconds per frame. Results were similar with 1,377 contours, with 94.6% of runs having completely optimal paths with the average run time of 5.2 s. For fewer than 500 cells, the algorithm runs almost instantaneously with optimal results. Thus, unlike other techniques, HOPS can be performed on a large number of neuronal targets in an imaged field of view. In our hands, successful scans with single-cell resolution have been performed on neuronal populations of up to 1,500 cells. This limit reflects our optical system and biology and is not intrinsic to the software's run time speed or scalability. To avoid the introduction of dead samples into scanning, HOPS continuously scans a closed path, thus eliminating the "flyback" time of the mirrors returning to the start point.

Acquisition. The TSP path and rig-specific mirror characterization data are then fed into our acquisition software that allows the user to acquire a fluorescence time series for a fixed amount of time or number of frames. In addition, acquisition can be triggered off of a transistor-transistor logic (TTL) event. During scanning, all PMT data for the entire on- and off-cell path is constantly streamed to disk in a raw binary floating point format, acquiring up to four samples for each mirror movement to account for and limit errors due to single sample shot noise.

Fluorescence signal expansion. After performing a scan, we address the possibility of having been too conservative in the characterization of mirror inertia for a fraction of the path segments. At the end of acquisition, cell boundaries are redefined based on an expansion of on-cell samples using a corridor around the mean fluorescence signal ± 2.75 SD while scanning over each cell (Fig. 2*D*). This step limits lost signal resulting from small micrometer-sized errors in contour generation or elliptical somatic shapes. After expansion of utilized signal, PMT traces are averaged with respect to cell identities and on-cell samples for each frame to produce a matrix of fluorescence values over imaging frames for all cells. Finally, the specific time in microseconds when each cell is sampled is calculated given the saved HOPS metadata.

Signal-to-Noise Consideration

After path creation, the user is able to set the number of samples to spend on each target. By dramatically decreasing the time spent scanning neuropil, the time spent sampling neuronal somatic fluorescence becomes a proportionally and significantly larger time of the total scan. As a result, a further increase in frame rate can be achieved by minimizing cell sampling duration. During a standard raster scan of a calcium indicator dye-loaded mouse brain slice, an average of 4.19% of the time is spent measuring neuronal fluorescence (1.18-mm^2 scanned area; $n = 62$ fields of view containing 614 ± 152 neurons). By minimizing the path, HOPS increases the percentage of time spent sampling the desired neuronal signal to an average of 42.15% of the total scan. We constrained and limited this time by empirically evaluating the number of samples necessary to detect sufficient fluorescent signal indicative of a single action potential within an imaged neuron (Fig. 3*A*). We found, using combined imaging and whole cell electrophysiology calibration experiments (25 μM fura-2 pentapotassium salt dye), that 16 samples (50.0 μs) per neuron per frame easily achieves a signal-to-noise ratio (SNR) sufficient to resolve a single action potential in a cell

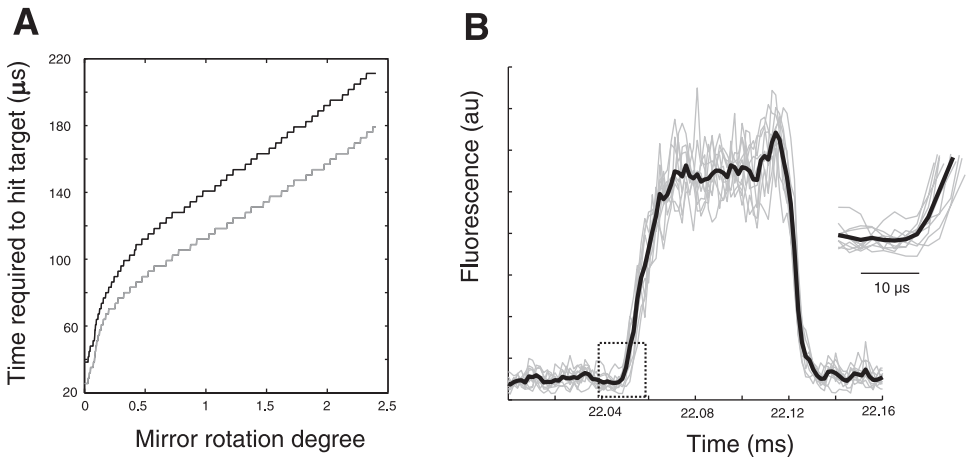

Fig. 4. Characterizing mirror response allows precise and stable long-term fluorescence recording. *A*: the duration of mirror rotation differs for the *X* (shaded) and *Y* (solid) galvanometers. *B*: the resulting scan path is extremely stable over a prolonged period. Fluorescence measures corresponding to frames 1, 200, 400, . . . , 1,800 are shown (shaded), and the average of these 10 traces (solid) is overlaid. *Inset*: the path enters the neuron at the same sample, i.e., within ±3.12 μs, each time. In this example, the total frame duration was 84.93 ms and the total scan time was 152.88 s.

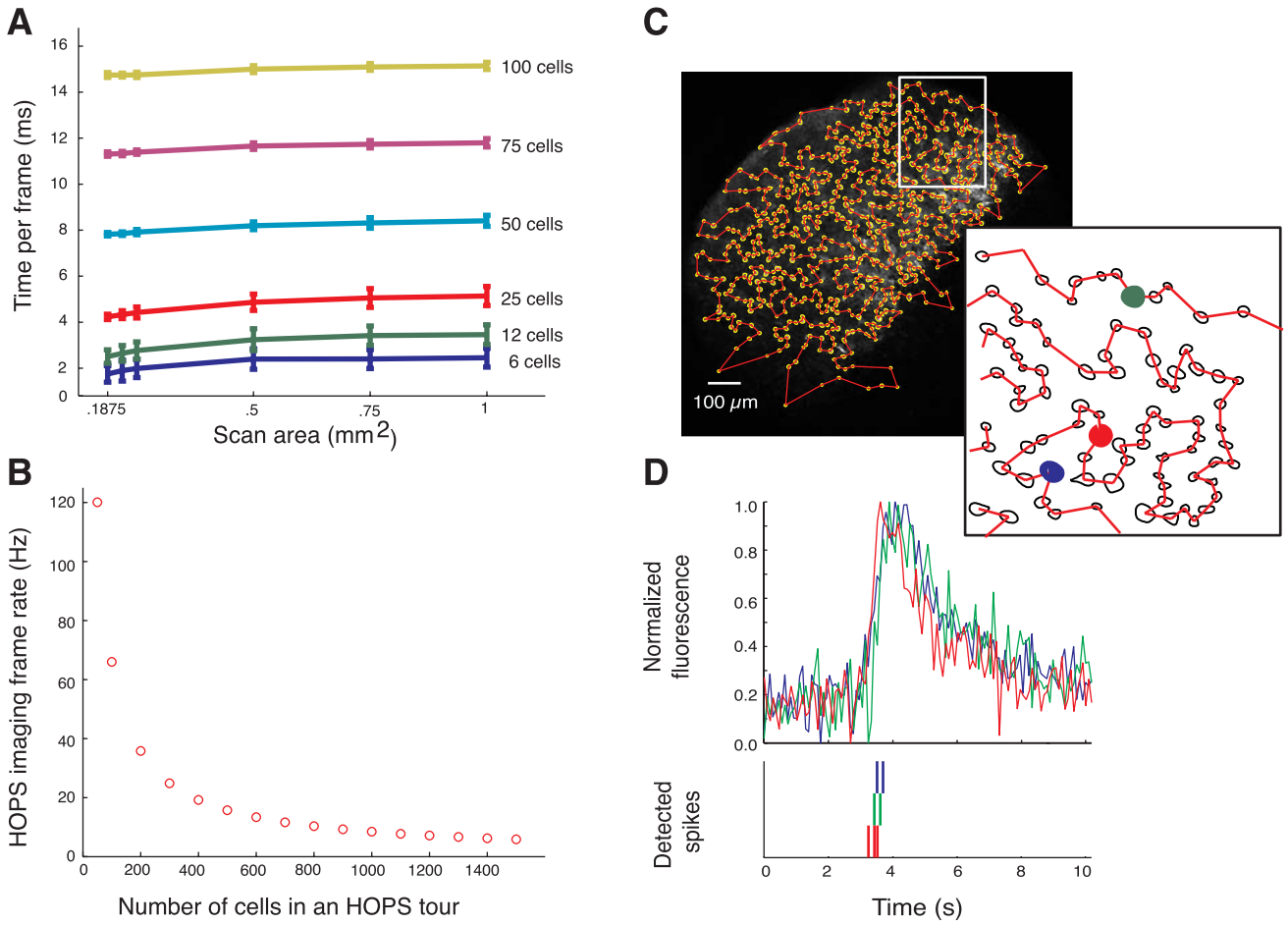

Fig. 5. HOPS provides high scan rates that are faster than traditional MPLSM scanning and have little dependence on the area of the field of view. *A*: the duration of each frame is mainly determined by the number of neurons scanned and not the area covered by the scan. Values are means; error bars indicate ±SD. *B*: mean scan rate given varying numbers of uniformly distributed neurons ($n = 25$ for each point) in a 1.18-mm^2 field of view. *C*: MPLSM of fura-2 AM-loaded neurons in a slice of mouse somatosensory cortex. Bright punctuate areas are cell somata. Optimal laser scan path between automatically detected neurons (yellow) is illustrated by the thin red line. *Inset*: an expansion of the HOPS path. *D*: examples of fluorescence measures corresponding to circuit activity in the 3 representative neurons (red, green, and blue) from the expansion of *C* and the modeled most likely spike train given these fluorescence changes.

within a field with as few as 50 (Fig. 3*B*) or as many as 1,000 neurons (Fig. 3*C*). For different HOPS tour durations, different concentrations of dye, or different dyes such as genetically encoded calcium indicators, the number of samples necessary to detect single action potentials will likely vary. In addition, the number of samples necessary also depends on the number of neurons scanned. For example, small populations are being scanned, single-action potential resolution can also be achieved using only two samples per cell, increasing scan rates from ~150 Hz at 16 samples to ~250 Hz given 50 cells. To account for these variables, HOPS allows the user to define the number of samples spent on each target in the scan path depending on the fluorophore and the experimental design, balancing the maximization of the frame rate and SNR.

Mirror Characterization

An optimal linear path does not ensure either prolonged path stability or accurate fluorescent measures from each individual neuron. The galvanometric mirror system has nonlinear inertia-based responses to any given set of voltage commands. Thus it is critical to allow the galvanometers sufficient time to reach each neuron on every iteration of the path, ensuring stable fluorescence measures over prolonged periods. To maximize frame rate while also maintaining spatial interframe stability with single-sample (3.12 μs) precision, we empirically generated a lookup table that

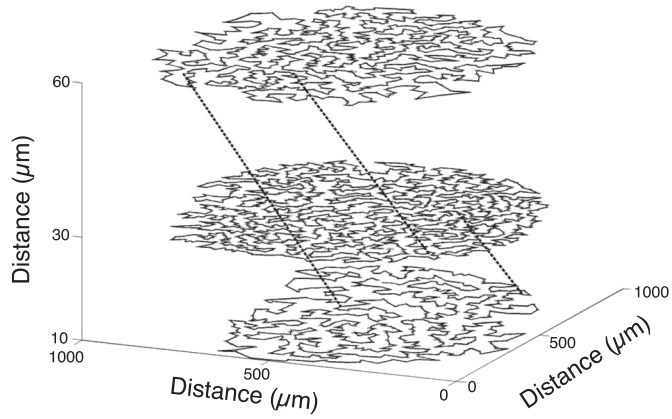

Fig. 6. HOPS can been scaled to 3 dimensions. Adding a piezo stepper motor and using multiple 2-dimensional planes of cell selection and HOPS path creation further increases the number of recordable neurons. Dotted lines indicate piezo/mirror plane shifts.

converts target-to-target distance into the upper bound time (μs) necessary for both the *X* and *Y* mirrors to reach the next cell (Fig. 4, *A* and *B*). To construct these tables, we determined the time in microseconds required to reach various pollen grains or 15-μm-diameter microbeads at varying distances. Because the majority of between-cell distances are small, mirror movement is mainly restricted to the small rotation angle nonlinear regime. This lookup table, in addition to the mirror's own intrinsic acceleration control system, allows us to maximize scan time with respect to mirror inertia while also ensuring prolonged stability of fluorescent measures.

Imaging Speed

Given a worst case scenario of a uniform distribution of cells, across an 800 $\times$ 800-pixel field of view we are able to achieve scan rates of ~125 Hz for 50 neurons and ~8.5 Hz for 1,000 neurons, while optimizing the SNR considerations, compared with ~0.5 Hz for a raster scan (Fig. 5*A*). Given the clustering of neurons in an average field of view, it is likely that these scan rates are upper bounds to those achievable in experimental situations. The additional scan time imposed by an increase in scan area is minimal, since frame rate is mainly determined by the number of scanned targets and not by the area of the scan (Fig. 5*B*). Given the speed benefits of HOPS over a traditional galvanometer raster approach, large populations of cells can be simultaneously scanned while each cell's relative firing sequence is detected (Fig. 5*C*). The illustrated most likely spike train is modeled from the calcium fluorescence changes (Vogelstein et al. 2010) allowing for the detection of neuronal action potential sequences within and between cells. Note that our ability to detect action potential onset in a sequence is not confounded by the scan order.

DISCUSSION

HOPS allows the experimenter to make optimal use of a standard MPLSM setup for the rapid investigation of large-scale circuit sequences. HOPS is scalable to thousands of neuronal targets, is stable over prolonged and continuous imaging periods, and provides little overhead time, since it is fully automated. The method is modular and platform independent: any commercial or self-built MPLSM setup capable of generating raster images and providing independent voltage commands to the scan mirrors can utilize HOPS. From start to finish this entire process is fast, allowing a user to begin imaging using HOPS after an initial raster scan extremely quickly. The total computational time required to go from the generation of a field of view to starting a HOPS acquisition ranges from seconds with small numbers of cells to a minute with larger neuronal populations.

Similar to other MPLSM techniques (Cheng et al. 2011; Göbel et al. 2007), HOPS is also capable of being utilized in the axial or *Z* dimension, expanding its single-cell scanning possibilities to even larger populations of neurons (Fig. 6). The addition of a three-dimensional piezo stepper motor (model P-725.2CL; Physik Instrumente) allows focusing between different precise-depth two-dimensional planes as HOPS performs its scans. In this manner, HOPS allows an experimenter to scan cell bodies located at different depths in a slice of neuronal tissue.

The ability of software packages such as HOPS to modify the operation of galvanometric scanners to increase their scan speed provides a suitable alternative to purchasing faster scanning hardware or optical devices for multibeam scanning. In particular for in vitro slice and culture work, galvanometric scanners have the advantage of being able to provide scans over large angles of deflection, and therefore large numbers of cells, which, for example in the neocortex, span multiple layers and columns. As a result, HOPS allows researchers to address large-scale circuitry and fine-scale temporal structure questions using the standard MPLSM setup.

ACKNOWLEDGMENTS

We thank J. Waters, R. Yuste, B. Watson, V. Nikolenko, M. Runfeldt, and M. Vaidya for early assistance and helpful comments.

GRANTS

This work was supported by the Dana Foundation (J. N. MacLean), National Science Foundation CAREEER Award 0952686 (J. N. MacLean), National Institute of General Medical Sciences Grant GM007839 (A. J. Sadovsky), and Swiss National Science Foundation Grant PBBEP3-123668 (F. B. Neubauer).

DISCLOSURES

No conflicts of interest, financial or otherwise, are declared by the author(s).

REFERENCES

Amaral ME, Grant JR, Riggs PK, Stafuzza NB, Filho EA, Goldammer T, Weikard R, Brunner RM, Kochan KJ, Greco AJ, Jeong J, Cai Z, Lin G, Prasad A, Kumar S, Saradhi GP, Mathew B, Kumar MA, Miziara MN, Mariani P, Caetano AR, Galvão SR, Tantia MS, Vijh RK, Mishra B, Kumar ST, Pelai VA, Santana AM, Fornitano LC, Jones BC, Tonhati H, Moore S, Stothard P, Womack JE. A first generation whole genome RH map of the river buffalo with comparison to domestic cattle. *BMC Genomics* 9: 631, 2008.

Apiletti D, Baralis E, Cerquitelli T. Energy-saving models for wireless sensor networks. *Knowl Inf Syst*: 1–30, 2010.

Cheng A, Gonçalves JT, Golshani P, Arisaka K, Portera-Cailliau C. Simultaneous two-photon calcium imaging at different depths with spatio-temporal multiplexing. *Nat Methods* 8*:* 139–144, 2011.

Duemani Reddy G, Kelleher K, Fink R, Saggau P. Three-dimensional random access multiphoton microscopy for functional imaging of neuronal activity. *Nat Neurosci* 11: 713–720, 2008.

Fan GY, Fujisaki H, Miyawaki a Tsay RK, Tsien RY, Ellisman MH. Video-rate scanning two-photon excitation fluorescence microscopy and ratio imaging with cameleons. *Biophys J* 76: 2412–2420, 1999.

Göbel W, Kampa BM, Helmchen F. Imaging cellular network dynamics in three dimensions using fast 3D laser scanning. *Nat Methods* 4: 73–79, 2007.

Harris KD. Neural signatures of cell assembly organization. *Nat Rev Neurosci* 6: 399–407, 2005.

Hebb DO. *The Organization of Behavior*. New York: Wiley, 1949.

Helsgaun K. An effective implementation of the Lin-Kernighan traveling salesman heuristic. *Eur J Oper Res* 126: 106–130, 2000.

Kudrimoti HS, Barnes C, McNaughton BL. Reactivation of hippocampal cell assemblies: effects of behavioral state, experience, and EEG dynamics. *J Neurosci* 19: 4090–4101, 1999.

Lillis KP, Eng A, White JA, Mertz J. Two-photon imaging of spatially extended neuronal network dynamics with high temporal resolution. *J Neurosci Methods* 172: 178–184, 2008.

MacLean JN, Watson BO, Aaron GB, Yuste R. Internal dynamics determine the cortical response to thalamic stimulation. *Neuron* 48: 811–823, 2005.

Nikolenko V, Poskanzer KE, Yuste R. Two-photon photostimulation and imaging of neural circuits. *Nat Methods* 4: 943–950, 2007.

Nikolenko V, Watson BO, Araya R, Woodruff A, Peterka DS, Yuste R. SLM microscopy: scanless two-photon imaging and photostimulation with spatial light modulators. *Front Neural Circuits* 2: 1–14, 2008.

Ohki K, Chung S, Kara P, Hübener M, Bonhoeffer T, Reid RC. Highly ordered arrangement of single neurons in orientation pinwheels. *Nature* 442: 925–928, 2006.

Otsu Y, Bormuth V, Wong J, Mathieu B, Dugué GP, Feltz A, Dieudonné S. Optical monitoring of neuronal activity at high frame rate with a digital random-access multiphoton (RAMP) microscope. *J Neurosci Methods* 173: 259–270, 2008.

Valmianski I, Shih AY, Driscoll JD, Matthews DW, Freund Y, Kleinfeld D. Automatic identification of fluorescently labeled brain cells for rapid functional imaging. *J Neurophysiol* 104: 1803–1811, 2010.

Vogelstein JT, Packer AM, Machado TA, Sippy T, Babadi B, Yuste R, Paninski L. Fast non-negative deconvolution for spike train inference from population calcium imaging. *J Neurophysiol* 104: 3691–3704, 2010.

Watson BO, MacLean JN, Yuste R. UP states protect ongoing cortical activity from thalamic inputs. *PLoS One* 3: e3971, 2008.

Watson BO, Nikolenko V, Yuste R. Two-photon imaging with diffractive optical elements. *Front Neural Circuits* 3: 1–11, 2009.